12th IFAC International Symposium on
Advanced Control of Chemical Processes
July 14-17, 2024. Toronto, Canada

Simultaneous parameter estimation and state-estimator tuning for systems with nonstationary disturbances, multi-rate data and measurement delay

Qiujun A. Liu*, Kimberley B. McAuley*

** Department of Chemical Engineering, Queen's University, Canada, (e-mail: kim.mcauley@queensu.ca)*

Abstract: Model-based monitoring and control of chemical and biochemical processes rely on estimators like Extended Kalman Filters (EKFs) to ensure accurate predictions in real time. The selection of suitable model parameters and tuning factors is crucial for precise predictions. An extended Simultaneous Parameter Estimation and Tuning (SPET) method is proposed to handle complex systems with nonstationary disturbances, time-varying parameters, multi-rate data, and measurement delay. Through a case study on a Continuous Stirred Tank Reactor (CSTR), we demonstrate that SPET outperforms traditional approaches, achieving improved online predictions and state estimator performance.

Keywords: State estimator tuning, Extended Kalman filter, Parameter estimation, Stochastic process disturbances, Multi-rate sampling, Time-varying parameters, Measurement delay

1. INTRODUCTION

Model-based control and monitoring applications based on fundamental models have gained significant traction due to the popular concept of Digital Twins (Botín-Sanabria et. al., 2022). Accurate parameter estimates are crucial for the success of these applications. Relatively simple dynamic models are commonly used online for easier implementation and maintenance. However, these simplified models may not capture all complexities of the process, resulting in mismatch between model predictions and actual process behavior. To reduce mismatch, state estimators are used to update model predictions and time-varying parameters, while accounting for model imperfections and measurement noise. The Extended Kalman Filter (EKF) is one of the most popular state estimators used in Engineering fields such as polymerization and biochemical processes. due to its simplicity and robustness (Ogunnaike, 1994; Gudi, et al., 1994; Schneider and Georgakis, 2013). However, using EKFs and other state estimators to achieve accurate updates of model states relies on proper tuning. While traditional trial-and-error tuning may be adequate for simple models with few states and measurements, more systematic approaches are necessary as models become more complex (Odelson and Rawlings, 2006; Valappil and Georgakis, 2000). Moreover, challenges arise when implementing state estimators in complex situations involving nonstationary disturbances, multi-rate data, and measurement delays (Kozub and MacGregor, 1992; Gudi et. al., 1995; Gopalakrishnan et. Al., 2011). Recently, a new method has been proposed for estimating fixed model parameters and tuning of state estimators in these complex situations (Liu, 2023) and is presented here. This article is structured as follows. Section 2 provides information about EKFs. Section 3 presents the proposed extension of the SPET method. In Section 4, a nonlinear CSTR case study is used to demonstrate the effectiveness of SPET. Lastly, Section 5 provides conclusions.

2. PRELIMINARIES

The current article uses the standard EKF equations (Brown and Hwang, 1997) as presented in Table 1.

Table 1. Standard EKF equations

Discretized Nonlinear Model:

$$\boldsymbol{x}_k = \boldsymbol{F}(\boldsymbol{x}_{k-1}, \boldsymbol{u}_{k-1}, \boldsymbol{\theta}) + \boldsymbol{w}_k \quad (1)$$

$$\boldsymbol{y}_k = \boldsymbol{g}(\boldsymbol{x}_k, \boldsymbol{\theta}) + \boldsymbol{\varepsilon}_k \quad (2)$$

One-Step-Ahead Model Predictions:

$$\hat{\boldsymbol{x}}_{k+1|k} = \boldsymbol{F}(\hat{\boldsymbol{x}}_{k|k}, \boldsymbol{u}_k, \boldsymbol{\theta}) \quad (3)$$

$$\boldsymbol{P}_{k+1|k} = \boldsymbol{A}_k \boldsymbol{P}_{k|k} \boldsymbol{A}_k^T + \boldsymbol{Q}_k \quad (4)$$

State and Covariance Update Equations:

$$\hat{\boldsymbol{x}}_{k+1|k+1} = \hat{\boldsymbol{x}}_{k+1|k} + \boldsymbol{K}_{k+1}(\boldsymbol{y}_{k+1} - \boldsymbol{g}(\hat{\boldsymbol{x}}_{k+1|k}, \boldsymbol{\theta})) \quad (5)$$

$$\boldsymbol{K}_{k+1} = \boldsymbol{P}_{k+1|k} \boldsymbol{H}_{k+1}^T \left(\boldsymbol{H}_{k+1} \boldsymbol{P}_{k+1|k} \boldsymbol{H}_{k+1}^T + \boldsymbol{R}_k \right)^{-1} \quad (6)$$

$$\boldsymbol{P}_{k+1|k+1} = \boldsymbol{P}_{k+1|k} - \boldsymbol{K}_{k+1} \boldsymbol{H}_{k+1} \boldsymbol{P}_{k+1|k} \quad (7)$$

where

$$\boldsymbol{A}_k = \frac{\partial \boldsymbol{F}}{\partial \boldsymbol{x}} \Big|_{\hat{\boldsymbol{x}}_{k|k}}, \boldsymbol{H}_{k+1} = \frac{\partial \boldsymbol{g}}{\partial \boldsymbol{x}} \Big|_{\hat{\boldsymbol{x}}_{k+1|k}}$$

In Equation (1), the vector $\boldsymbol{x}_k \in R^X$ is the state vector at time t_k. The function $\boldsymbol{F} \in R^X$ contains solutions of differential equations representing the current states $\boldsymbol{x}_k$ in terms of previous states values $\boldsymbol{x}_{k-1}$, inputs $\boldsymbol{u}_{k-1}$ and model parameters $\boldsymbol{\theta}$. The vector $\boldsymbol{w}_k \in R^X$ denotes discrete stochastic model errors, assumed to be normally distributed with $\boldsymbol{w}_k \sim \boldsymbol{N}(\boldsymbol{0}, \boldsymbol{Q}_k)$, where $\boldsymbol{Q}_k$ is the discrete-white-noise model-error covariance matrix. Equation (2) relates the measurement vector $\boldsymbol{y}_k \in R^Y$ to the states $\boldsymbol{x}_k$ and possibly the model parameters $\boldsymbol{\theta}$ through the output functions $\boldsymbol{g} \in R^Y$. The vector $\boldsymbol{\varepsilon}_k \in R^Y$ contains measurement errors, also assumed to be normally disturbed with $\boldsymbol{\varepsilon}_k \sim \boldsymbol{N}(\boldsymbol{0}, \boldsymbol{R}_k)$, where $\boldsymbol{R}_k$ is the measurement-error covariance matrix. For the remaining

equations, the symbol ^ is used for estimated results and the symbol $\big|$ indicates "given" information. For example, the subscript $k+1\,\big|\,k$ refers to predictions at the sampling time $k+1$ while considering information from measurements at time k. $\boldsymbol{P}$ is the state-error covariance matrix; $\boldsymbol{K}$ is the Kalman gain matrix; $\boldsymbol{A_k}$ is the linearized state-transition matrix and $\boldsymbol{H}_k$ is the linearized measurement-transition matrix.

3. PROPOSED METHODOLOGIES

Using the proposed SPET methodology for EKFs in complex situations requires formulating the dynamic model with time-varying parameters and non-stationary disturbances as additional state variables. Multi-rate sampling is handled by adjusting $\boldsymbol{H}_k$. Further details are provided elsewhere (Liu, 2023). Observability is a crucial condition for the success of state-estimation algorithms as it enables determination of state variables based on the available inputs and outputs. The proposed methodology requires that sufficient measurements are available to ensure observability. Additional insights and comments on observability and its evaluation for the CSTR case study are provided by Liu (2023).

The SPET methodology was developed to simultaneously estimate fixed model parameters and the tuning parameters for state estimators. The first step of the SPET approach involves using the Laplace Approximation Maximum Likelihood Estimation (LAMLE) method (Karimi and McAuley, 2014; Liu et al., 2022) to estimate the model parameters $\boldsymbol{\theta}$, as well as the elements of the continuous process-error covariance matrix $\boldsymbol{Q_c}$ and the measurement-error covariance matrix $\boldsymbol{R}$. LAMLE is used to estimate $\boldsymbol{\zeta} = [\boldsymbol{\theta}^T, \boldsymbol{B}^T, \boldsymbol{R}_{\boldsymbol{diag}}^T, \boldsymbol{Q}_{\boldsymbol{c}\,\boldsymbol{diag}}^T]^T$, where $\boldsymbol{B}$ is a vector of B-spline coefficients for the estimated state trajectories and the subscript "$\boldsymbol{diag}$" refers to the diagonal elements of the covariance matrices. The decision variables in $\boldsymbol{\zeta}$ are obtained by minimizing the objective function:

$$
\begin{aligned}
&J_{LAMLE} \\
&= \frac{1}{2}\left(\sum_{r=1}^{Y} N_r ln\big(R_{y_r}\big)\right) + \frac{q}{2}\left(\sum_{s=1}^{X} ln\big(Q_{x_s}\big)\right) \\
&+ \frac{[\boldsymbol{Y_m} - \boldsymbol{g_m}(\boldsymbol{x}_{\sim}, \boldsymbol{u}, \boldsymbol{\theta})]^T \boldsymbol{\Sigma_R^{-1}} [\boldsymbol{Y_m} - \boldsymbol{g_m}(\boldsymbol{x}_{\sim}, \boldsymbol{u}, \boldsymbol{\theta})]}{2} \\
&+ \frac{\sum_{i=1}^{q} \boldsymbol{w}^T\, \boldsymbol{Q_c^{-1}} \Delta t^{-1}\, \boldsymbol{w}}{2} + ln\det\big(\boldsymbol{H}_{\boldsymbol{x}_{\sim}}\big),
\end{aligned}
\tag{8}
$$

where

$$\boldsymbol{w} = \boldsymbol{x}_{\sim}(t_i) - \boldsymbol{x}_{\sim}(t_{i-1}) - \boldsymbol{f}(\boldsymbol{x}_{\sim}(t_{i-1}), \boldsymbol{u}(t_{i-1}), \boldsymbol{\theta})\Delta t$$

In Equation (8), the subscript ~ is used to indicate B-spline approximations for the state trajectories. The first two terms involve the diagonal elements R_{y_r} and Q_{x_s} in matrices $\boldsymbol{R}$ and $\boldsymbol{Q_c}$, respectively. Here, N_r is the number of measurements for the r^{th} response variable, and q is the total number of discrete time points where random disturbances are assumed to enter the system. The third term involves the residuals between the stacked vector of measurements $\boldsymbol{Y_m}$ and the stacked vector of predictions $\boldsymbol{g_m}$, weighted by $\boldsymbol{\Sigma_R}$, which is an error covariance matrix for the stacked measurements. The fourth term considers the weighted residuals between the estimated state trajectories and their predictions. The last term involves a Hessian matrix $\boldsymbol{H}_{\boldsymbol{x}_{\sim}}$ containing second derivatives with respect to the spline coefficients in $\boldsymbol{B}$ (Liu et al., 2022). Estimating $\boldsymbol{\zeta}$ from Equation (8) using gradient-based optimization methods is difficult, because analytical derivatives of $ln\,det(\boldsymbol{H}_{\boldsymbol{x}_{\sim}})$ with respect to the elements in $\boldsymbol{\zeta}$ are prohibitively complicated. To address this challenge, an iterative two-step process was developed to avoid complicated derivative calculations (Karimi and McAuley, 2014; Liu et al., 2022).

Previously, the SPET method was developed for systems where all measurements are sampled with the same frequency and without delay (Liu et al., 2021). SPET was used to estimate $\boldsymbol{\theta}$, $\boldsymbol{Q_c}$, $\boldsymbol{R}$ and $\boldsymbol{\Sigma_\theta}$ via LAMLE and then to obtain $\boldsymbol{Q}_k$ and $\boldsymbol{R}_k$, the tuning parameters for EKF's implementation:

$$\boldsymbol{Q}_k = \boldsymbol{A}_{\boldsymbol{\theta}\,k} \boldsymbol{\Sigma_\theta} \boldsymbol{A}_{\boldsymbol{\theta}\,k}^T + \boldsymbol{Q_c}\Delta t, \tag{9}$$

where

$$\boldsymbol{A}_{\boldsymbol{\theta}\,k} = \frac{\partial \boldsymbol{F}}{\partial \boldsymbol{\theta}}\Big|_{\hat{\boldsymbol{x}}_{k|k'}\hat{\boldsymbol{\theta}}} = \begin{bmatrix} \frac{\partial F_1}{\partial \theta_1} & \cdots & \frac{\partial F_1}{\partial \theta_P} \\ \vdots & \ddots & \vdots \\ \frac{\partial F_X}{\partial \theta_1} & \cdots & \frac{\partial F_X}{\partial \theta_P} \end{bmatrix}\Big|_{\hat{\boldsymbol{x}}_{k|k'}\hat{\boldsymbol{\theta}}}$$

$$\boldsymbol{R}_k = \boldsymbol{H}_{\boldsymbol{\theta}\,k} \boldsymbol{\Sigma_\theta} \boldsymbol{H}_{\boldsymbol{\theta}\,k}^T + \boldsymbol{R}, \tag{10}$$

where

$$\boldsymbol{H}_{\boldsymbol{\theta}\,k} = \frac{\partial \boldsymbol{g}}{\partial \boldsymbol{\theta}}\Big|_{\hat{\boldsymbol{x}}_{k|k'}\hat{\boldsymbol{\theta}}} = \begin{bmatrix} \frac{\partial g_1}{\partial \theta_1} & \cdots & \frac{\partial g_1}{\partial \theta_P} \\ \vdots & \ddots & \vdots \\ \frac{\partial g_X}{\partial \theta_1} & \cdots & \frac{\partial g_X}{\partial \theta_P} \end{bmatrix}\Big|_{\hat{\boldsymbol{x}}_{k|k'}\hat{\boldsymbol{\theta}}}$$

In Equation (9), $\boldsymbol{A_\theta}$ contains partial derivatives of the system functions $\boldsymbol{F}$ with respect to the parameters $\boldsymbol{\theta}$, and Δt is the sampling interval. Notice that, this expression for $\boldsymbol{Q}_k$ accounts for stochastic disturbances and for uncertainties in model predictions due to parameter uncertainties $\boldsymbol{\Sigma_\theta}$. Similarly, Equation (10) for the measurement-error covariance matrix $\boldsymbol{R}_k$ takes in to account the potential influence of parameter uncertainties on the predicted outputs in $\boldsymbol{g}$.

In the current article, the SPET method is extended to handle more complex scenarios with nonstationary disturbances, time-varying parameters, delay, and multi-rate measurements. In the first step of the algorithm, LAMLE is used to estimate $\boldsymbol{\theta}$, $\boldsymbol{Q_c}$, $\boldsymbol{R}$ and $\boldsymbol{\Sigma_\theta}$ from historical data. This estimation process is performed offline, which allows delayed measurements to be handled by shifting them backward in time. Unlike the earlier development of SPET, which assumed simple stationary Gaussian process disturbances (Liu et. al., 2021), the extended framework considers more complex process noise structures. This allows for the modeling of sustained shifts in process behavior by incorporating time-varying parameter states $\boldsymbol{x}^{\theta}$, and additive nonstationary process disturbances $\boldsymbol{x}^{ns}$ in addition to the regular states $\boldsymbol{x}^{f}$ that arise from fundamental balances. The formulation of the SDE process models becomes:

$$\dot{\boldsymbol{x}}^f(t) = \boldsymbol{f}\big(\boldsymbol{x}^f(t), \boldsymbol{x}^{\theta}(t), \boldsymbol{u}(t), \boldsymbol{\theta}\big) + \boldsymbol{x}^{ns}(t) \tag{11}$$

$$\dot{\boldsymbol{x}}^{\theta}(t) = \mathbf{0} + \boldsymbol{\eta}^{\theta}(t) \tag{12}$$

$$\dot{\boldsymbol{x}}^{ns}(t) = \mathbf{0} + \boldsymbol{\eta}^{ns}(t) \tag{13}$$

So that, the corresponding $\boldsymbol{Q_c}$ is:

$$\boldsymbol{Q_c} = \begin{bmatrix} \mathbf{0} & \mathbf{0} & \mathbf{0} \\ \mathbf{0} & \boldsymbol{Q_c^{\theta}} & \mathbf{0} \\ \mathbf{0} & \mathbf{0} & \boldsymbol{Q_c^{ns}} \end{bmatrix} \tag{14}$$

Note that Equations (11) and (13) assume perfect material and energy balance equations when variations in $\boldsymbol{x}^{\theta}$ and $\boldsymbol{x}^{ns}$ are considered. As a result, matrix $\boldsymbol{Q_c}$ in Equation (14) contains zeros as diagonal elements at the top left. During the estimation of $\boldsymbol{Q_c}$, $\boldsymbol{\theta}$ and $\boldsymbol{R}$ using LAMLE, these zero elements of $\boldsymbol{Q_c}$ are already known and do not require estimation. However, this situation introduces a divide-by-zero issue in the LAMLE objective function (Equation (8)), because $\boldsymbol{Q_c^{-1}}$ appears as a weighting factor. To resolve this issue, Liu et al., (2022) suggested replacing the zero diagonal elements with very small values. This approach ensures the invertibility of $\boldsymbol{Q_c}$, while indicating that the material and energy balances are accurate and should be enforced during LAMLE parameter estimation. Further details on how to use LAMLE results to tune and implement EKFs systems with time-varying parameters, nonstationary disturbances, multi-rate data and measurement delays are provided by Liu (2023).

4. CASE STUDY

A CSTR case study first developed by Marlin (2000) has been augmented with stochastic terms to account for nonstationary disturbances and time-varying parameters as shown in Table 2. This case study is used to demonstrate and evaluate the proposed extensions to SPET.

Table 2. SDE model for CSTR

$$\frac{dC_A}{dt} = \frac{F(t)}{V}\big(C_{A0}(t) - C_A(t)\big) - k_r(T)C_A(t) = f_1\big(x_1(t), x_2(t), k_{ref}(t), u(t), \theta\big) \tag{15}$$

$$\frac{dT}{dt} = \frac{F(t)}{V}\big(T_0(t) - T(t)\big) + \gamma k_r(T)C_A(t) - UA(F_c)\big(T(t) - T_{cin}(t)\big) + M(t) = f_2\big(x_1(t), x_2(t), k_{ref}(t), M(t), u(t), \theta\big) \tag{16}$$

$$\frac{dk_{ref}}{dt} = \eta_{k_{ref}}(t) \tag{17}$$

$$\frac{dM}{dt} = \eta_M(t) \tag{18}$$

$$UA(F_c) = \frac{aF_c^{b+1}}{V\rho C_p\left(F_c + \frac{aF_c^b}{2\rho_c C_{pc}}\right)} \tag{19}$$

$$\gamma = -\frac{\Delta H_{rxn}}{\rho c_p} \tag{20}$$

$$k_r(T) = k_{ref}\exp\left(-\frac{E}{R}\left(\frac{1}{T} - \frac{1}{T_{ref}}\right)\right) \tag{21}$$

$$y_C\big(t_{mC,j}\big) = C_A\big(t_{mC,j} - 2.0\big) + \varepsilon_C\big(t_{mC,j}\big) \quad \text{for } j = 0 \dots n_C \tag{22}$$

$$y_T\big(t_{mT,j}\big) = T\big(t_{mT,j}\big) + \varepsilon_T\big(t_{mT,j}\big) \quad \text{for } j = 0 \dots n_T \tag{23}$$

The concentration of reactant A, C_A, and the reactor temperature, T, are fundamental process states. Equation (15) is a material balance on the reactant, and Equation (16) is an energy balance on liquid in the reactor. The process inputs $\boldsymbol{u} = [F, C_{A0}, T_0, T_{cin}, F_c]^T$ include the feed flow rate F, feed concentration C_{A0}, feed temperature T_0, inlet coolant temperature T_{cin}, and coolant flow F_c. Figure 1 shows input trajectories used in a typical simulated dynamic experiment. True parameter values and model constants used to generate synthetic data are shown in Tables 3 and 4.

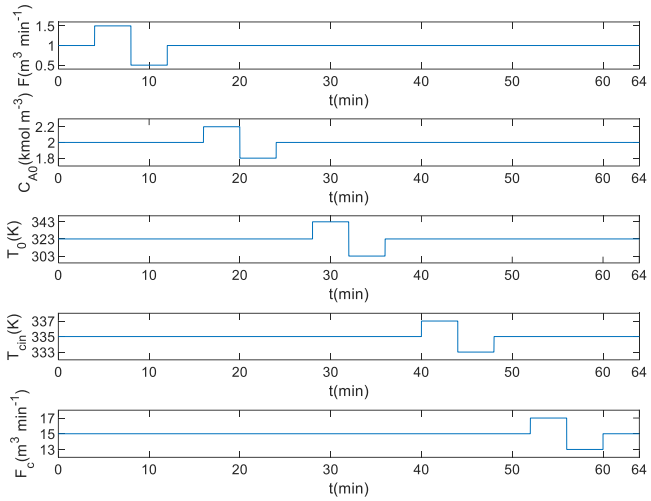

Figure 1. Input trajectories used to generate simulated dynamic data

Table 3. Simulation parameters

Parameter	True Value	Units
E/R	8.3301×10^{3}	K
a	1.678×10^{6}	-
b	0.5	-
$Q_{c_{k_{ref}}}$	2.5×10^{-5}	min^{-3}
Q_{c_M}	0.5	$\text{K}^2\ \text{min}^{-3}$
R_C	4×10^{-4}	$\text{kmol}^2\ \text{m}^{-6}$
R_T	0.25	K^2

Table 4. Model constants

Description	Symbol	Value	Units
Heat capacity of reactor contents	C_p	1	cal $\text{g}^{-1}\ \text{K}^{-1}$
Heat capacity of coolant	C_{pc}	1	cal $\text{g}^{-1}\ \text{K}^{-1}$
Reference temperature	T_{ref}	340	K
Volume of the reactor	V	1	m^3
Density of reactor contents	ρ	10^6	g m^{-3}
Density of coolant	ρ_c	10^6	g m^{-3}
Enthalpy of reaction	ΔH_{rxn}	-130×10^{6}	cal kmol^{-1}

In Equation (15), the material balance contains a time-varying rate constant k_{ref}, which accounts for unknown impurities and poorly understood side reactions not explicitly modeled. This parameter is treated as an additional nonstationary state (as $x_3 = k_{ref}$), and its dynamics are influenced by a stationary stochastic disturbance $\eta_{k_{ref}}$, as shown in Equation (17). To address uncertainties in the energy balance, an additive stochastic mismatch term M is included. This nonstationary disturbance captures uncertainties that are due to heat loss to the environment, fouling in the cooling coil, and viscosity changes in the reactor liquid. In Equation (18), M is driven by stationary stochastic disturbance η_M. Measurement equation (22) accounts for a 2.0-minute time delay in the concentration measurement, while Equation (23) assumes no delay in the temperature measurement. Measurement noise is taken into account through the inclusion of ε_C and ε_T in Equations (22) and (23), respectively. It is assumed that stationary stochastic disturbances $\eta_{k_{ref}}$ and η_M, as well as the measurement errors ε_C and ε_T, follow white Gaussian distributions and are independent, so that the continuous process error covariance matrix $\boldsymbol{Q_c}$ and the measurement error covariance matrix $\boldsymbol{R}$ are:

$$\boldsymbol{Q_c} = \begin{bmatrix} 0 & 0 & 0 & 0 \\ 0 & 0 & 0 & 0 \\ 0 & 0 & Q_{c_{k_{ref}}} & 0 \\ 0 & 0 & 0 & Q_{c_M} \end{bmatrix} \tag{24}$$

$$\boldsymbol{R} = \begin{bmatrix} R_C & 0 \\ 0 & R_T \end{bmatrix} \tag{25}$$

The continuous stochastic disturbances $\eta_{k_{ref}}$ and η_M are included in the simulated data using discrete noise with a time interval of $\Delta t = 0.2$ min (Varziri et. al., 2008). In simulated experiments, the concentration is measured every 1.0 minute, resulting in a total of 64 measurements per experiment (n_C = 64), and temperature measurements are taken more frequently at intervals of 0.2 minutes, resulting in n_T = 320.

A total of 600 sets of simulated experimental data were generated using the CSTR SDE model, with each set corresponding to a different random noise sequence. Out of these, 500 data sets were used for estimating model parameters and tuning parameters and 100 were used for EKF testing.

4..1 Simultaneous parameter estimation and tuning (SPET) for the CSTR system

LAMLE was first used to estimate the elements of $\boldsymbol{\zeta} = \left[a, b, \frac{E}{R}, \boldsymbol{B}^T, \boldsymbol{R}_{\boldsymbol{diag}}^T, \boldsymbol{Q}_{\boldsymbol{c}\,\boldsymbol{diag}}^T\right]^T$ and to determine the covariance matrix $\widehat{\boldsymbol{\Sigma}}_{\boldsymbol{\theta}}$ for the model parameters. In some cases, practitioners may have multiple batches of historical data instead of just one. In this case study, five batches of historical data were used for each set of estimated parameters. As a result, the LAMLE objective function for the five batches was:

$$J_{LAMLE,multi} = \sum_{m=1}^{5} J_{LAMLE,m} \tag{26}$$

where $J_{LAMLE,m}$ is obtained from the right-hand side of Equation (8) for each batch of data.

Diagonal elements of the discrete model-error covariance matrix $\widehat{\boldsymbol{Q}}_k$ were determined using Equation (9) as follows:

$$\begin{bmatrix} \hat{Q}_C \\ \hat{Q}_T \\ \hat{Q}_{k_{ref}} \\ \hat{Q}_M \end{bmatrix}_k = \boldsymbol{A}_{\boldsymbol{\theta}\,k} \widehat{\boldsymbol{\Sigma}}_{\boldsymbol{\theta}}\, \boldsymbol{A}_{\boldsymbol{\theta}\,k}^T + \begin{bmatrix} 0 \\ 0 \\ \hat{Q}_{c_{k_{ref}}} \\ \hat{Q}_{c_M} \end{bmatrix} \Delta t \tag{27}$$

Since the output functions of the CSTR are independent of the parameters, the measurement-error covariance matrix is time invariant:

$$\widehat{\boldsymbol{R}}_k = \widehat{\boldsymbol{R}} = \begin{bmatrix} \hat{R}_C \\ \hat{R}_T \end{bmatrix} \tag{28}$$

Details on how to set the initial state covariance matrix $\boldsymbol{P}_{0|0}$, and how to the formulate the discretized dynamic model to account for extra states arising due to the time-varying parameter k_{ref}, nonstationary disturbance M and ten periods of measurement delay are provided elsewhere (Liu, 2023).

4.2 Results and discussion

Estimated model parameters and tuning factors were obtained using SPET and a more conventional approach where the model parameters were first obtained using weighted least squares (WLS) estimation. Using WLS, fixed values of k_{ref} and M were estimated along the other model parameters. In the conventional approach, the diagonal elements of $\widehat{\boldsymbol{Q}}_k$ were obtained by minimizing the sum of squared innovations (SSI) based on the 5 batches of historical data used for parameter estimation. The SPET and conventional WLS+SSI estimates and tuning factors were then used to implement EKFs with new online data.

Figures 2 and 3 compare the performance of both approaches for one-step ahead predictions and updated states, respectively. The results demonstrate that both approaches perform well, as they closely align with the measured values and true trajectories. On average, the SPET approach yields superior results compared to the WLS+SSI approach for this specific test run (Run 80).

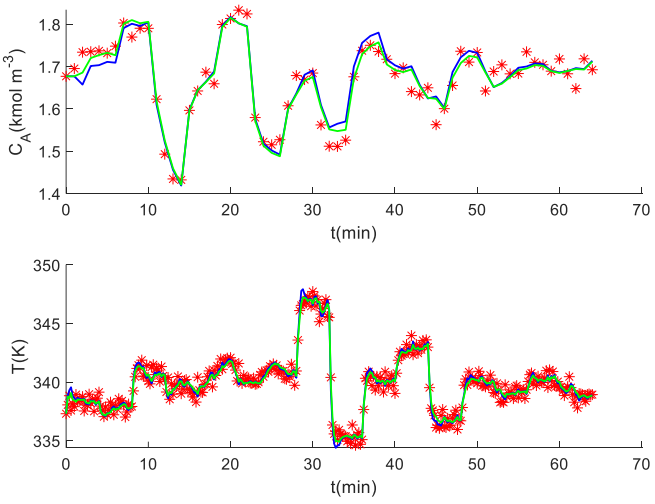

Figure 2. Measurements (∗) and one-step-ahead predictions using SPET (—) and WLS+SSI (—)

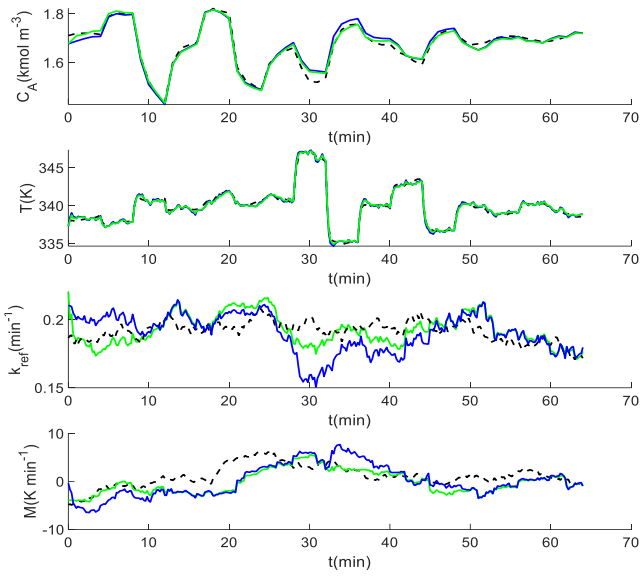

Figure 3. True trajectories (▪▪▪) and updated state estimates using SPET (—) and WLS+SSI (—) approaches for Test Run 80

The performance of the EKFs is summarized in Figure 4, which shows the sum-of-squared prediction errors (SSPE) and sum-of-squared state errors (SSSE) for the 100 sets of test data. Equations used for computing SSPE and SSSE for C_A and T as shown in the boxplots in Figure 4 are:

$$SSPE_C = \sum_{j=1}^{N_C} \left(y_C(t_{mC,j}) - \hat{C}_p(t_{mc,j} - 2.0)\right)^2 \quad (29)$$

$$SSSE_C = \sum_{j=1}^{N_C} \left(C(t_{mC,j}) - \hat{C}(t_{mC,j})\right)^2 \quad (30)$$

where $\hat{C}_p(t_{mc,j} - 2.0) = \hat{C}_{d10\,5j|5j-1}$ and $\hat{C}(t_{mC,j}) = \hat{C}_{5j|5j}$

$$SSPE_T = \sum_{j=1}^{N_T} \left(y_T(t_{mT,j}) - \hat{T}_p(t_{mT,j})\right)^2 \quad (31)$$

$$SSSE_T = \sum_{j=1}^{N_T} \left(T(t_{mT,j}) - \hat{T}(t_{mT,j})\right)^2 \quad (32)$$

where $\hat{T}_p(t_{mT,j}) = \hat{T}_{j|j-1}$ and $\hat{T}(t_{mT,j}) = \hat{T}_{j|j}$

Figure 4 also shows the results of a "True" scenario, which serves as an ideal benchmark for comparison. In the "True" scenario, perfect model parameter values and tuning factors were used, to show the best possible performance that could be achieved by an EKF with noisy new data. The results clearly demonstrate the effectiveness of the SPET-based EKF, which performs almost as well as a perfectly tuned EKF with perfect model parameters. Moreover, the average SSPE and SSSE of C_A for the SPET approach are 11% and 42% better, respectively than for the WLS+SSI approach. As shown in Figure 4, the medians of the SPET and the WLS+SSI approaches are similar (with SPET having slightly smaller medians), but the inter-quartile ranges (IQRs) for SPET are smaller than those of the WLS+SSI approach. The smaller IQR values indicates that the SPET results are more robust to random measurement error and stochastic process disturbances. One possible factor contributing to the superior EKF performance achieved with SPET, compared to WLS+SSI, is the improved estimation of model parameters (better median and smaller IQRs), as shown in Figure 5. Considering the nonstationary states k_{ref} and M during LAMLE parameter estimation led to improved estimates of parameters a, b and E/R compared to assuming that k_{ref} and M were time invariant during WLS parameter estimation.

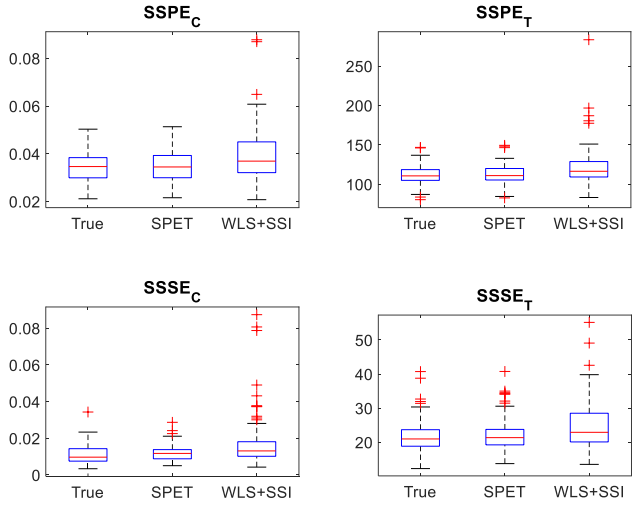

Figure 4. Boxplots for EKF performance using SPET and WLS+SSI

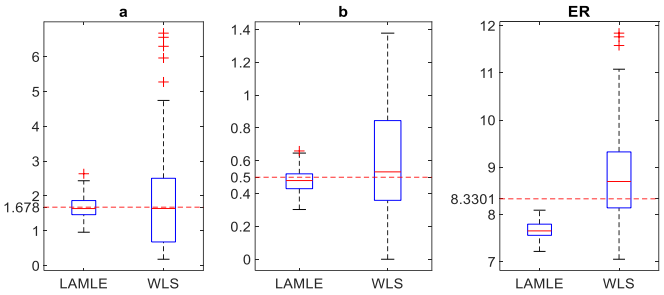

Figure 5. Boxplots for estimates of model parameters using LAMLE and WLS, true parameter values (---)

Additional scenarios considered by Liu (2023) reveal that benefits of using SPET compared to conventional WLS+SSI are obtained when data sets of different sizes are available for estimating model and tuning parameters. In situations where the modeler has prior knowledge about some or all of the model parameters in $\boldsymbol{\theta}$, the LAB (Laplace Approximation Bayesian) method (Karimi and McAuley, 2018) can be applied instead of LAMLE. This Bayesian approach can be particularly useful when dealing with small historical data sets or data sets with too little excitation to estimate all the model parameters without prior knowledge. We anticipate that the advantages of the SPET approach will become more beneficial in larger parameter and state-estimation problems, although further testing is necessary to validate this hypothesis.

While using SPET, we have identified a potential concern related to the computational time required. Specifically, the

off-line estimation of model parameters from 5 batches of historical data using LAMLE took approximately 2 hours on a Lenovo ThinkPad X280 computer, whereas the WLS+SSI approach only required ~20 minutes. This difference in computational time could become more significant for larger-scale systems, where the computational requirements of SPET may become burdensome. However, it is worth noting that this issue can be addressed by improving the implementation of the optimization algorithm. By improving the algorithm's efficiency, the computational time for SPET can be reduced in future, making it more attractive for larger-scale systems. Testing of the algorithm using large systems is an important next step.

5. CONCLUSIONS

In conclusion, this article has focused on the development and improvement of state estimation techniques for chemical and biochemical processes, specifically targeting the use of EKFs in complex situations involving nonstationary disturbances, time-varying parameters, multi-rate data, and measurement delays. The Simultaneous Parameter Estimation and Tuning (SPET) method has been extended to address these complexities effectively. Through testing using a nonlinear CSTR case study, the results have demonstrated the superiority of the SPET approach over the traditional sequential approach employing weighted least squares (WLS) for parameter estimation and minimizing squared innovation terms for EKF tuning using historical data. The extended SPET method has achieved more accurate and reliable online model predictions and state estimates, resulting in significant improvements in average sum-of-squared prediction errors and sum-of-squared state errors, specifically a reduction of 6% and 42%, respectively, for the delayed concentration in the tested scenario.

Furthermore, the proposed SPET methodology holds great potential for advanced state estimators such as Moving Horizon Estimators (MHEs), Unscented Kalman Filters (UKFs), and Ensemble Kalman Filters (EnKFs), which all benefit from accurate model parameters and reliable estimates of process and measurement noise covariances. To further validate and explore the capabilities of the SPET methodology, future work should involve testing it on larger systems and real process data. The continuous development of formal methods for tuning EKFs, especially in complex situations, will contribute to the advancement of state estimation techniques in chemical and biochemical engineering.

REFERENCES

Botín-Sanabria, D.M., Mihaita, A.S., Peimbert-García, R.E., Ramírez-Moreno, M.A., Ramírez-Mendoza, R.A. and Lozoya-Santos, J.D.J. (2022). Digital twin technology challenges and applications: A comprehensive review. *Remote Sensing*, 14(6), p.1335.

Brown, R.G., and Hwang, P.Y.C. (1997). *Introduction to Random Signals and Applied Kalman Filtering: With MATLAB Exercises and Solutions.* New York: Wiley.

Gopalakrishnan, A., Kaisare, N.S. and Narasimhan, S. (2011). Incorporating delayed and infrequent measurements in Extended Kalman Filter based nonlinear state estimation. *Journal of Process Control*, 21(1), pp.119-129.

Gudi, R.D., Shah, S.L. and Gray, M.R. (1995). Adaptive multirate state and parameter estimation strategies with application to a bioreactor. *AIChE Journal*, 41(11), pp.2451-2464.

Karimi, H. and McAuley, K.B. (2014). A maximum-likelihood method for estimating parameters, stochastic disturbance intensities and measurement noise variances in nonlinear dynamic models with process disturbances. *Computers & chemical engineering*, 67, pp.178-198.

Karimi, H. and McAuley, K.B. (2018). Bayesian objective functions for estimating parameters in nonlinear stochastic differential equation models with limited data. *Industrial & Engineering Chemistry Research*, 57(27), pp.8946-8961.

Kozub, D.J. and MacGregor, J.F. (1992). State estimation for semi-batch polymerization reactors. *Chemical Engineering Science*, 47(5), pp.1047-1062.

Liu, Q.A., Karimi, H. and McAuley, K.B. (2021). Estimating uncertainties and parameters for fundamental models used in online monitoring and control. *The Canadian Journal of Chemical Engineering*, 99(6), pp.1268-1287.

Liu, Q.A., Varshney, D. and McAuley, K.B. (2022). Parameter and uncertainty estimation in stochastic differential equation models with multi-rate data and nonstationary disturbances. *Chemical Engineering Research and Design*, 183, pp.118-133.

Liu, Q.A., (2023). *Simultaneous Parameter Estimation and State-Estimator Tuning for Fundamental Models*. Doctoral thesis, Queen's University, Kingston.

Marlin, T.E. (2000). *Process control: designing processes and control systems for dynamic performance*. McGraw-Hill Science, Engineering & Mathematics.

Odelson, B.J., Lutz, A. and Rawlings, J.B. (2006). The autocovariance least-squares method for estimating covariances: application to model-based control of chemical reactors. *IEEE transactions on control systems technology*, 14(3), pp.532-540.

Ogunnaike, B.A. (1994). On-line modelling and predictive control of an industrial terpolymerization reactor. International Journal of Control, 59(3), 711-729.

Schneider, R. and Georgakis, C. (2013). How to not make the extended Kalman filter fail. *Industrial & Engineering Chemistry Research*, 52(9), pp.3354-3362.

Valappil, J. and Georgakis, C. (2000). Systematic estimation of state noise statistics for extended Kalman filters. *AIChE Journal*, 46(2), pp.292-308.

Varziri, M.S., McAuley, K.B. and McLellan, P.J. (2008). Parameter estimation in continuous-time dynamic models in the presence of unmeasured states and nonstationary disturbances. *Industrial & engineering chemistry research*, 47(2), pp.380-393.